Use of Raman Forward Scatter for Seeding a Plasma Amplifier

Contact *james.sadler@physics.ox.ac.uk*

J. D. Sadler*, L. Ceurvorst, M. F. Kasim
N. Ratan, A. Savin, A. Ross, P. Norreys (PI)
Clarendon Laboratory,
University of Oxford, Parks Road,
Oxford, OX1 3PU

**These authors contributed equally*

K. Glize*, R. M. G. M. Trines, R. Bingham,
N. Bourgeois, D. Symes, R. Pattathil
Central Laser Facility
STFC Rutherford Appleton Laboratory,
Didcot, OX11 0QX

F. Keeble
University College London, Gower Street,
London, WC1E 6BT

Experimental Facility: Astra Target Area 2

Plasma Raman amplifiers are under worldwide investigation as a possible successor to chirped pulse amplification. Compression of long laser pulses to bandwidth limited duration is of primary concern for high power laser facilities, however continued progress is currently limited by damage thresholds on solid state optics. Compression in a plasma will reduce the size and cost, and also allows effective compression of ultra-violet pulses. Experimental progress has been hampered by the need for a high power seed pulse with wavelength approximately 10% longer than the long uncompressed pulse. Here we test a pre-amplifier stage, using plasma Raman forward scatter, to easily generate the required seed. This forward scatter agrees with high resolution Particle-in-Cell simulations.

Introduction

Amplification of a laser pulse in plasma has received considerable attention since the 1990s, with the potential to vastly increase the maximum available on-target intensity compared to solid state amplifiers. With current chirped pulse amplification (CPA) systems, the pulse is stretched and chirped before the amplifier chain, to avoid damaging intensities. To increase the power, the pulse is then re-compressed to its bandwidth limited duration. However, the complex solid state optics suffer damage and require periodic replacement, even with pulse intensity and fluence limitations.

Analytical models [1-4] have shown how a long pulse may be compressed with energy efficiency 50% and compression ratio over 10^4 in an under-dense plasma. Subsequent large scale particle-in-cell and Vlasov simulations [5,6] have verified the high efficiency. The mechanism is Raman backward scattering, which occurs through the beating of two counter-propagating laser pulses. The pulse frequencies are chosen to resonantly excite an electron plasma wave, which scatters the long pump pulse to amplify the lower frequency short pulse. Although the simulations show the scheme has great potential, experimental progress has been slow mainly due to the unavailability of a suitable down-tuned seed pulse [7,8]. This proof of concept experiment shows how plasma Raman forward scatter from a primary plasma stage could be suitable for seeding a backwards secondary amplifier.

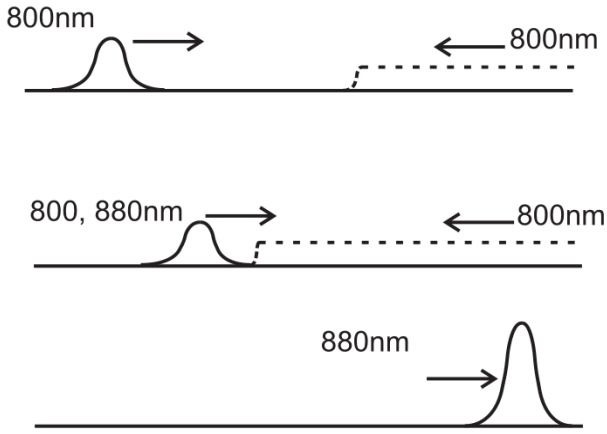

Fig. 1 Schematic of the backwards Raman amplifier scheme, with seeding from forward scatter of a short pulse, in a plasma approximately 1/100 of critical density. The experiment used the shorter pulse only, to assess its effectiveness as a seed, however the full scheme was simulated using the Particle-in-Cell code Osiris.

Experimental Set-up

The proposal is illustrated in Fig. 1. Firstly, a high intensity pulse of frequency ω ionises a plasma channel of around 1/100 critical density and undergoes spontaneous Raman scatter. Some of this forward scattered light at frequency $\omega - \omega_p$ (where ω_p is the plasma frequency) will propagate through the secondary plasma stage of identical density. Here a long, lower intensity pump pulse of frequency ω counter-propagates, amplifying the seed light through stimulated Raman backward scatter. This technique allows the plasma pre-amplifier stage to take care of generating high power seed radiation at the correct frequency.

As a proof of concept, the pre-amplifier stage was tested using the Astra laser at the Central Laser Facility. The main beam arrived at target from a f/17 parabolic mirror with duration 45 fs, energy 353 mJ ± 10% and spot diameter 29 μm, ionising a methane plasma from a 3 mm gas jet target. This gives a dimensionless peak amplitude of $a_0 = 0.7 \pm 12\%$. Diagnostics included exit mode imaging, spectroscopy of the forward scattered light, low magnification transverse Mach-Zehnder interferometry and GRENOUILLE reconstruction of the forward scatter intensity envelope.

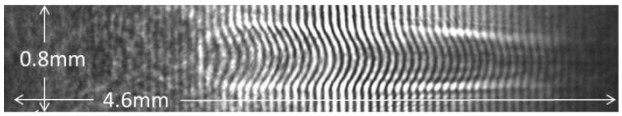

Fig. 2 Transverse interferometry data using the Astra probe pulse at 800 nm, centred on the gas jet. The phase shift was extracted in the centre and Abel inverted, giving an on axis electron density of $1.3 \times 10^{19}/\mathrm{cm}^3 \pm 16\%$ or $0.0075 n_{crit}$. The error was estimated by comparing the imaging resolution to the fringe shift.

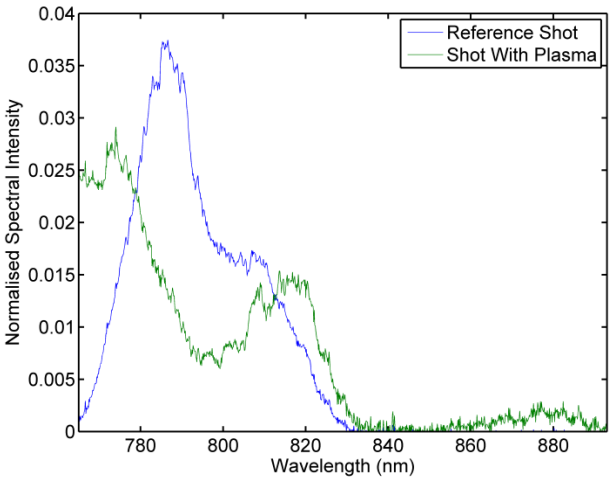

Fig. 3 Spectrometer data, corrected for transmission and sensitivity, for a reference shot with no plasma and a shot with electron density of $1.3 \times 10^{19}/\mathrm{cm}^3$. The red-shifted Raman peak is around 880 nm.

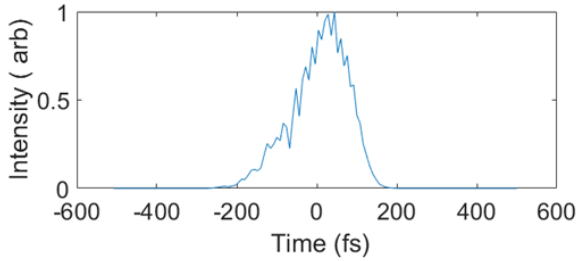

Fig. 4 Inversion of the Grenouille diagnostic data, giving the intensity envelope as a function of time. A long pass filter was used to block light below 850 nm.

Results

Fig. 2 shows the plasma channel from the transverse interferometry diagnostic, using a 40 fs, 800 nm probe pulse passing transversely through the plasma channel. Due to the relativistic mass increase of electrons within the laser pulse, the resonant plasma frequency is altered. The expected Raman forward scatter frequency is $\omega - \omega_p/\sqrt{\gamma}$, where
$\gamma = < \sqrt{1 + a_0^2 \, (\mathbf{sin}\, \omega t)^2} > \approx 1 + a_0^2/4$
is the mean Lorentz factor for the quiver motion of an electron, where the expansion is approximately valid for $a_0 < 1$.

Fig. 3 shows the full aperture spectrum collected in the forwards direction. The fundamental light has one blue shifted peak from the electron density gradient at the ionisation front and one red shifted peak from the wakefield gradient. In addition, there is a Raman scattering peak with central wavelength 878 nm. The spectrum has been corrected for the transmission of optics and the CCD sensitivity. The observed Raman forward scatter wavelength is consistent with the expected value (from the independent density measurement) of 876 nm without the relativistic correction, or 871 nm with the relativistic correction. The wide observed bandwidth of the Raman light $\frac{\delta\omega}{\omega} = 0.035$ is explained by the high intensity interaction. Linear theory indicates the bandwidth of the Raman light is of the order of the growth rate [9] $\gamma/\omega = a_0\sqrt{n/n_{crit}} = 0.05$.

Imaging the forward scattered Raman light showed a slight misalignment with the incoming beam, possibly due to a density gradient due to use of a tilting gas jet. Imaging the Raman light and integrating the signal was therefore a more accurate energy measurement than the spectrometer. 8.0% of the incoming pump energy was contained above a wavelength 850 nm, a measurement obtained using a long pass filter with cutoff wavelength 850 nm.

The forward scattered light above 850 nm was also directed to a Grenouille diagnostic to measure the phase and intensity as a function of time, shown in Fig.4. The output appears as a relatively smooth single pulse, although lengthened compared to the initial drive pulse due to the group velocity mismatch in the plasma and long pass filter. The short duration of the output is important as several computational studies have found that the most effective seeds are short in duration, shorter than the linear Raman growth time.

The diagnostics show a usable seed pulse is developed. However, it was found that generating enough light to seed the secondary amplifier requires a high intensity short pulse to start with. It is therefore unlikely that a subsequent backwards amplification stage could improve on this initial pulse power. This is because the Raman amplification scheme saturates when the amplified pulse reaches relativistic intensity. This is due to de-tuning caused by the dependence of the plasma frequency on a_0 and competing plasma instabilities that scale strongly with a_0, such as ponderomotive filamentation. However, a series of plasma amplifier stages with increasing beam size could vastly improve on the initial short pulse power.

The output pulse still had large spectral components around 800 nm which will not be resonant in the secondary stage and will hinder rather than seed the amplifier. These spectral components will not be amplified but will co-propagate with the amplified light and degrade the pulse through further spontaneous Raman scattering and ponderomotive filamentation. Unless this detrimental part of the spectrum could be selectively filtered out before the main amplifier stage, it will stimulate detrimental parametric instabilities.

Particle-in-Cell Simulation

A one-dimensional particle-in-cell simulation is now compared to the experimental results. The simulation used the code Osiris with 62 cells and 7,700 particles per wavelength, in a simulation window of length 500 μm that moved with the drive beam. A 45 fs, bandwidth limited Gaussian pulse with peak dimensionless amplitude 0.64 and central wavelength 790 nm propagated through a uniform plasma of electron density $1.3 \times 10^{19}/\mathrm{cm}^3$. Atoms were initially neutral and ionised through a field ionisation model for hydrogen. Neutralising ions were kept static. The spectrum of the pulse after 1 mm of propagation was found to closely match the experiment. It is shown in Fig. 5.

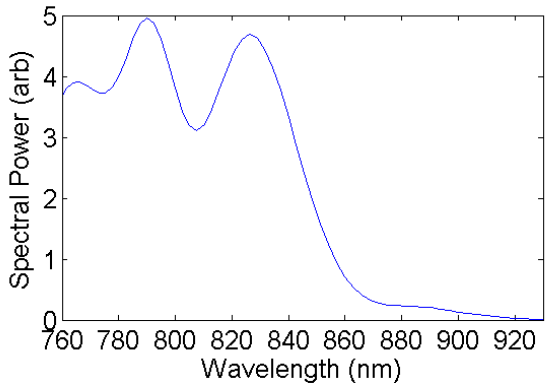

Fig. 5 Simulated spectrum of the main pulse after 1 mm of propagation.

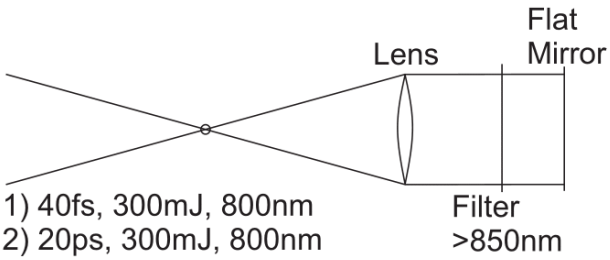

Fig. 6 Possible arrangement to filter out unwanted light below 850 nm. Around 30 mJ of forward scatter (as measured in the experiment) from the gas target would propagate through the spectral filter and be focussed back in to the target, overlapping with a second longer pulse with a suitable delay to overlap through the target. In this way a high power, ultra-short seed pulse and a high energy pump pulse may be generated using the same laser system. Reflective optics may also be used to minimise the seed pulse duration.

The spectrum exhibits the blue and red shifted peaks of the main pulse, as well as a non-zero signal at the Raman peak around 880 nm. The positions and relative amplitude of the peaks are similar to the experiment, however they appear slightly broader. The spectrum above 860 nm contains 1.5% of the initial energy.

To simulate the full scheme, the simulation continued for a further 4 mm with a counter propagating long pulse of wavelength 800 nm and constant dimensionless amplitude 0.03 entering from the front of the simulation box. Although some spectral components were amplified, the pulse lengthened, lost coherence and broke up. Further analysis suggested that the large amount of remaining spectral power around 800 nm in the short pulse was stimulating competing plasma instabilities, giving the output limited applicability. The simulation was repeated with a lower intensity short pulse of $a_0 = 0.05$, however there was no discernible Raman forward scattering above the level of the noise in the simulation, suggesting the problem cannot be countered in this way.

One possible solution is to expand the beam and use spectral filters to select only the Raman scattering peak above 850 nm, a setup already implemented for the Grenouille diagnostic. Refocusing the remaining light through the target would then provide an effective seed pulse. A possible arrangement is shown in Fig. 6. In this way, the seed and pump pulse may be generated using the same laser system and a high power seed pulse around 880 nm easily generated using Raman forward scattering. Using this high fidelity seed, a series of plasma amplifier stages could amplify it to petawatt power level using easily available 800 nm terawatt pump pulses.

Conclusions

In summary, the experiment showed that a promising amount of seed light for a Raman amplifier could easily be generated through Raman forward scattering in a pre-amplifier stage. It had ultra-short duration, energy around 30 mJ and repeatable characteristics. Simulations showed that the accompanying fundamental light must first be filtered out. This technique enables a high power femtosecond seed pulse and a high energy pump pulse to be generated with the same laser system.

Acknowledgements

This work has been carried out within the framework of the EUROfusion Consortium and has received funding from the Euratom research and training programme 2014-2018 under grant agreement No 633053. This work has also been funded by EPSRC grant number EP/L000237/1 and by STFC grant number ST/M007375/1. The authors would like to thank the Osiris consortium and the staff of the Central Laser Facility and Scientific Computing Department at STFC Rutherford Appleton Laboratory. This work used the ARCHER UK National Supercomputing Service (http://www.archer.ac.uk) and STFC's SCARF cluster.

References

1. V. M. Malkin, G. Shvets and N. J. Fisch, Phys. Rev. Lett. **82**, 4448 (1999)
2. J. P. Farmer, B. Ersfield and D. A. Jaroszynski, Phys. Plasmas **17**, 113301 (2010)
3. N. A. Yampolsky and N. J. Fisch, Phys. Plasmas **18**, 056711 (2011)
4. V. M. Malkin, G. Shvets and N. J. Fisch, Phys. Rev. Lett. **84**, 1208 (2000)
5. R. M. G. M. Trines *et al.*, Nat. Phys. **7**, 87 (2011)
6. Z. Toroker, V. M. Malkin and N. J. Fisch, Phys. Plasmas **21**, 113110 (2014)
7. J. Ren *et al.*, Nat. Phys. **3,** 732, (2007)
8. Y. Ping *et al.* Phys. Rev. Lett. **92**, 175007 (2004)
9. W. L. Kruer, "The Physics of Laser Plasma Interactions", (1988)